Numerical studies of spin-wave dynamics in Heisenberg spin-glasses

W. Y. Ching
Department of Physics, University of Missouri-Kansas City, Kansas City, Missouri 64110

D. L. Huber and K. M. Leung*
Department of Physics, University of Wisconsin, Madison, Wisconsin 53706
(Received 7 November 1980)

We outline the numerical techniques used in calculating the one-magnon zero-temperature dynamic structure factor of a Heisenberg spin-glass. We employ equation-of-motion methods to study the dynamics of the Edwards-Anderson model where the exchange integral between nearest neighbors has a Gaussian distribution with zero mean and no correlation between different bonds. Numerical results are presented for a $16 \times 16 \times 16$ simple cubic lattice with periodic boundary conditions. No evidence is found for long-wavelength propagating modes. A fit to the data suggests that at small q the structure factor is peaked at $E = 0$. The methods are completely general and can be applied to other Heisenberg systems provided the exchange integrals and equilibrium spin orientations of the corresponding classical Hamiltonian are available as input.

I. INTRODUCTION

In recent years increasing attention has been paid to the study of the low-lying excitations in Heisenberg magnets showing spin-glass behavior. It is generally believed that a universal feature of such systems is the existence of a large number of quasidegenerate "ground-state" configurations. At the risk of some oversimplification the low-lying modes can be divided into two categories: small amplitude oscillations relative to a given equilibrium configuration, which we refer to as "spin waves," and transitions between equilibrium configurations, which can take place either through tunneling or by means of thermal excitation.

Little is known about the second category of excitations. However considerable progress has been made in the analysis of the spin waves. Walker and Walstedt[1,2] were the first to carry out a systematic investigation of spin-wave modes in a Heisenberg spin-glass. They found equilibrium configurations (EC's) by successively rotating each spin into the direction of its local field, the procedure being carried to the point where the energy stabilized. Harmonic spin waves were obtained by linearizing the equations of motion for the spins, treating deviations from the equilibrium orientations as small parameters. In this way they were able to set up a dynamical matrix. From the eigenvalues and eigenvectors of the dynamical matrix they calculated the density of states and the localization indices. They first applied the analysis to *Cu*Mn[1,2] and subsequently to *Au*Fe.[2] The present authors have used the same approach in investigating the spin-wave modes in the Edwards-Anderson model,[3] where the exchange interactions have a Gaussian distribution, *Pd*Mn,[4] $Eu_xSr_{1-x}S$,[5] and most recently in an fcc antiferromagnetic with nearest-neighbor interactions.[6]

Up to now the most meaningful tests of the validity of the approach of Walker and Walstedt have come from comparisons between the measured and calculated values of the specific heat. In the cases of *Cu*Mn,[1,2] *Au*Fe,[2] *Pd*Mn,[4] and $Eu_xSr_{1-x}S$,[5] the contribution from the harmonic spin waves dominates the magnetic specific heat at temperatures $T \lesssim \frac{1}{2} T_f$, where T_f is the spin-glass freezing temperature as determined from the peak in the uniform field susceptibility. Evidence in support of the importance of harmonic spin waves is also provided by a comparison with the experimental values of the zero-temperature reversible susceptibility. Good agreement is obtained for both *Cu*Mn and *Au*Fe.[1,2] The results obtained for the specific heat and susceptibility in the various systems seem to show that the interconfiguration excitations have a negligible effect on the thermal properties at low temperatures, although presumably such excitations do play a role in the relaxation of the remanent magnetization.

Aside from information about the degree of localization the approach based on matrix diagonalization has provided little insight into the nature of the spin-wave modes. An important question raised some time ago[7,8] concerns the existence of weakly damped, long-wavelength propagating modes. Information about the dyamic response and thus the possible existence of such modes can be obtained from a study of the dynamic susceptibility, $S(\vec{q},E)$, which is probed in inelastic neutron scattering measurements. In principle $S(\vec{q},E)$ can be calculated from the eigenvectors and eigenvalues of the dynamical matrix.

However calculations done this way are limited to comparatively small systems, $\lesssim 200$ spins, and thus give no information about the response of the system to long-wavelength disturbances.

Because of this limitation calculations of $S(\vec{q},E)$ have been carried out by other methods. In Refs. 3–6 use was made of equation-of-motion techniques originally developed by Alben and Thorpe[9,10] for disordered ferromagnets and antiferromagnets. More recently Krey[11,12] has calculated $S(\vec{q},E)$ for $Eu_xSr_{1-x}S$ using continued fraction methods. Both the continued fraction and the equation-of-motion techniques can be applied to much larger systems (10^3-10^4 spins) than can be studied by direct diagonalization. However they have the drawback that they become increasingly less accurate as $E\rightarrow 0$, which is the region of interest for the problem of the propagating modes.

The purpose of this paper is to provide the detailed description of the application of equation-of-motion techniques to the study of the low-lying excitations in spin-glasses which had been outlined in Ref. 3. The use of the method is illustrated taking as an example the Edwards-Anderson (EA) model of a Heisenberg spin-glass.[13] We carry out calculations with larger samples than were employed in Ref. 3. Although our analysis pertains to spin-glasses our methods are applicable to spin systems with arbitrary interactions provided the EC's are known. The equation-of-motion methods are developed in Sec. II and applied to the EA model in Sec. III. Section IV is devoted to a discussion of our results.

II. EQUATION-OF-MOTION METHOD

In this section we develop the formalism of the equation-of-motion method for calculating the dynamic structure factor. The starting point in the analysis is the Heisenberg Hamiltonian which we write as

$$H=-\frac{1}{2}\sum_{j,k}J_{jk}\vec{S}^j\cdot\vec{S}^k \ , \tag{2.1}$$

where J_{jk} is the exchange integral and $\vec{S}^j$ is the spin ($j=1,\ldots,N$). We assume then an equilibrium configuration (EC) has been obtained which is specified by the set of unit vectors $\{\hat{\gamma}_j\}$ pointing in the directions of the equilibrium orientations of the $\vec{S}^j$. We introduce local Cartesian coordinate systems characterized by the triad of orthogonal unit vectors $(\hat{a}_j,\hat{b}_j(=\hat{\gamma}_j\times\hat{a}_j),\hat{\gamma}_j)$ and use the Holstein-Primakoff transformation to relate the components of $\vec{S}$ along the local coordinate axes to the boson annihilation and creation operators X_j and $X_j^\dagger$.

It is shown in Ref. 2 that the linearized equations of motion for X_j and $X_j^\dagger$ take the form ($\hbar=1$)

$$i\frac{dX_j}{dt}=\sum_k R_{jk}X_k^\dagger+\sum_k S_{jk}X_k \ , \tag{2.2}$$

$$i\frac{dX_j^\dagger}{dt}=-\sum_k R_{jk}^*X_k-\sum_k S_{jk}^*X_k^\dagger \ , \tag{2.3}$$

where the asterisk denotes complex conjugate. If we introduce the vectors $\vec{u}_j^{\pm}=\hat{a}_j\pm i\hat{b}_j$ then the matrices R_{jk} and S_{jk} are written

$$R_{jk}=-\tfrac{1}{2}SJ_{jk}\vec{u}_j^{+}\cdot\vec{u}_k^{+} \ , \tag{2.4}$$

$$S_{jk}=-\tfrac{1}{2}SJ_{jk}\vec{u}_j^{+}\cdot\vec{u}_k^{-}+\delta_{jk}S\sum_n J_{jn}\hat{\gamma}_j\cdot\hat{\gamma}_n \ . \tag{2.5}$$

As discussed below the dynamic structure factor can be expressed in terms of commutators of the form $\langle[S_x(\vec{q},t),S_x(-\vec{q},0)]\rangle$ where the angular brackets denote expectation values with respect to the EC and

$$S_x(\vec{q},t)=\sum_j\exp(-i\vec{q}\cdot\vec{r}_j)S_x^j(t) \ , \tag{2.6}$$

$\vec{r}_j$ being the position of the jth spin. In (2.6) S_x^j refers to the x component of $\vec{S}^j$ in the laboratory frame. It is related to the boson operators by means of the equation

$$\begin{aligned}S_x^j&\cong(S/2)^{1/2}(X_j+X_j^\dagger)\hat{x}\cdot\hat{a}_j-i(S/2)^{1/2}(X_j-X_j^\dagger)\hat{x}\cdot\hat{b}_j\\&\cong(S/2)^{1/2}(u_{jx}^{-}X_j+u_{jx}^{+}X_j^\dagger) \ ,\end{aligned} \tag{2.7}$$

where $u_{jx}^{\pm}$ denotes the x component of $\hat{u}_j^{\pm}$ in the laboratory frame. The symbol $\cong$ signifies that the right-hand side of (2.7) is the projection of the spin fluctuations in the plane perpendicular to $\hat{\gamma}_j$ on to the laboratory x axis. It is this projection which gives rise to the one-magnon contribution to the dynamic structure factor. It should be noted that $\sum_j(\vec{u}_jX_j+\vec{u}_j^{+}X_j^\dagger)$ is a constant of the motion for the harmonic spin-wave Hamiltonian, which is a consequence of the fact that $\sum_j\vec{S}_j$ commutes with the Heisenberg Hamiltonian.[14]

With the help of (2.7) we can write the correlation function in the one-magnon approximation in the form

$$\begin{aligned}\langle[S_x(\vec{q},t),S_x(-\vec{q},0)]\rangle=\tfrac{1}{2}S\sum_{j,k}\exp(-i\vec{q}\cdot\vec{r}_{jk})\{&u_{jx}^{-}u_{kx}^{-}\langle[X_j(t),X_k(0)]\rangle+u_{jx}^{+}u_{kx}^{+}\langle[X_j^\dagger(t),X_k^\dagger(0)]\rangle\\&+u_{jx}^{-}u_{kx}^{+}\langle[X_j(t),X_k^\dagger(0)]\rangle+u_{jx}^{+}u_{kx}^{-}\langle[X_j^\dagger(t),X_k(0)]\rangle\} \ ,\end{aligned} \tag{2.8}$$

where $\vec{r}_{jk}=\vec{r}_j-\vec{r}_k$.

By making use of the completeness relation for the eigenstates of the harmonic spin-wave Hamiltonian it is

readily shown that

$$\langle [X_j^\dagger(t),X_k^\dagger(0)]\rangle = -\langle [X_j(t),X_k(0)]\rangle^* \ , \tag{2.9}$$

$$\langle [X_j^\dagger(t),X_k(0)]\rangle = -\langle [X_j(t),X_k^\dagger(0)]\rangle^* \ . \tag{2.10}$$

Using (2.9) and (2.10) we obtain the result

$$\langle [S_x(\vec{q},t),S_x(-\vec{q},0)]\rangle = iS\sum_{j,k}\exp(-i\vec{q}\cdot\vec{r}_{jk})\,\mathrm{Im}\{u_{jx}^+u_{kx}^+\langle [X_j^\dagger(t),X_k^\dagger(0)]\rangle + u_{jx}^-u_{kx}^+\langle [X_j(t),X_k^\dagger(0)]\rangle\},$$

$$= iS\,\mathrm{Im}\left[\sum_{j,k}\exp(-i\vec{q}\cdot\vec{r}_{jk})\{u_{jx}^+u_{kx}^+\langle [X_j^\dagger(t),X_k^\dagger(0)]\rangle + u_{jx}^-u_{kx}^+\langle [X_i(t).X_k^\dagger(0)]\rangle\}\right] \ , \tag{2.11}$$

where Im denotes the imaginary part and we have made use of the assumed property that the sum over j and k is unchanged when $\vec{q}$ is replaced by $-\vec{q}$.

In the zero-temperature limit the xx component of the dynamic structure factor for positive frequencies can be expressed as

$$S_{xx}(\vec{q},E) = \frac{1}{2\pi}\int_{-\infty}^{\infty} dt\, e^{-iEt}\langle [S_x(\vec{q},t),S_x(-\vec{q},0)]\rangle \ . \tag{2.12}$$

The inelastic neutron scattering cross section in the harmonic approximation is related to (2.12) by a detailed balance factor, viz.,

$$\frac{d^2\sigma}{d\Omega\, dE} \propto \frac{S_{xx}(\vec{q},E)}{1-\exp(-E/k_BT)} \ . \tag{2.13}$$

Denoting the eigenstates by $|\nu\rangle$ and the EC by $|0\rangle$ we can write

$$\langle 0|S_x(\vec{q},t)S_x(-\vec{q},0)|0\rangle = \sum_\nu |\langle 0|S_x(\vec{q})|\nu\rangle|^2\exp(-i\omega_\nu t) \ , \tag{2.14}$$

where ω_ν is the energy of the excited state. Likewise we have

$$\tfrac{1}{2}\langle [S_x(\vec{q},t),S_x(-\vec{q},0)]\rangle = -i\sum_\nu |\langle 0|S_x(\vec{q})|\nu\rangle|^2\sin\omega_\nu t \ , \tag{2.15}$$

which when inserted into (2.12) leads to

$$S_{xx}(\vec{q},E) = \frac{2}{\pi}\int_0^\infty dt\sum_\nu |\langle 0|S_x(\vec{q},0)|\nu\rangle|^2\sin(\omega_\nu t)\sin(Et) = \frac{i}{\pi}\int_0^\infty dt\sin(Et)\langle [S_x(\vec{q},t),S_x(-\vec{q},0)]\rangle \ . \tag{2.16}$$

Equations (2.11) and (2.16) relate the dynamic structure factor to the microscopic properties of the Hamiltonian. However they are not in a form which is convenient for numerical analysis. A form which is convenient is obtained by introducing the Green's functions $G_{j\alpha}^{(1)}(\vec{q},t)$ and $G_{j\alpha}^{(2)}(\vec{q},t)$, $\alpha = x,y,z$, which are defined by

$$G_{j\alpha}^{(1)}(\vec{q},t) = \frac{1}{N}\sum_l \langle [X_j(t),X_l^\dagger(0)]\rangle\exp(i\vec{q}\cdot\vec{r}_l)u_{l\alpha}^+ \ , \tag{2.17}$$

and

$$G_{j\alpha}^{(2)}(\vec{q},t) = \frac{1}{N}\sum_l \langle [X_j^\dagger(t),X_l^\dagger(0)]\rangle\exp(i\vec{q}\cdot\vec{r}_l)u_{l\alpha}^- \ . \tag{2.18}$$

In light of (2.2) and (2.3) these functions obey the equations

$$i\frac{d}{dt}G_{j\alpha}^{(1)}(\vec{q},t) = \sum_k R_{jk}G_{k\alpha}^{(2)}(\vec{q},t) + \sum_k S_{jk}G_{k\alpha}^{(1)}(\vec{q},t) \ , \tag{2.19}$$

$$i\frac{d}{dt}G_{j\alpha}^{(2)}(\vec{q},t) = -\sum_k R_{jk}^*G_{k\alpha}^{(1)}(\vec{q},t) - \sum_k S_{jk}^*G_{k\alpha}^{(2)}(\vec{q},t) \ , \tag{2.20}$$

with the initial conditions

$$G_{j\alpha}^{(1)}(\vec{q},t=0) = N^{-1}\exp(i\vec{q}\cdot\vec{r}_j)u_{j\alpha}^+ \ , \tag{2.21}$$

$$G_{j\alpha}^{(2)}(\vec{q},t=0) = 0 \ . \tag{2.22}$$

Making use of Eqs. (2.16) – (2.18) we finally have

$$S_{\alpha\alpha}(\vec{q},E) = -\frac{S}{\pi}\int_0^\infty dt\sin(Et)\,\mathrm{Im}\left[\sum_j\exp(-i\vec{q}\cdot\vec{r}_j)[u_{j\alpha}^-G_{j\alpha}^{(1)}(\vec{q},t) + u_{j\alpha}^+G_{j\alpha}^{(2)}(\vec{q},t)]\right] \ , \tag{2.23}$$

which is the principal result of this section.

III. APPLICATION TO THE EDWARDS-ANDERSON MODEL

The approach outlined in Sec. II is applicable to arbitrary EC's. All that is needed are the exchange integrals and the vectors $\hat{\gamma}_j$ characterizing the equilibrium orientations of the spins. The matrices R_{jk} and S_{jk} are constructed according to (2.4) and (2.5) with $\vec{u}_j^{\pm} = \hat{a}_j \pm i\hat{b}_j$. The vectors $\hat{a}_j$ can be chosen arbitrarily subject to the conditions $\hat{a}_j^2 = 1$, $\vec{a}_j \cdot \vec{\gamma}_j = 0$. The dynamic structure factor is given by (2.23) with the Green's functions obtained by numerically integrating (2.19) and (2.20) with initial conditions (2.21) and (2.22). In order to avoid spurious oscillations associated with the finite interval of integration it is necessary to introduce a cutoff factor into the integrand in (2.23), i.e.,

$$\int_0^{\infty} dt\,(\cdots) \rightarrow \int_0^{T} dt\, e^{-\alpha t}(\cdots) \ , \tag{3.1}$$

with α such that $\exp(-\alpha T) \ll 1$.

We have applied the equation-of-motion techniques to the Edwards-Anderson (EA) model of a Heisenberg spin-glass.[3,13] The spins occupied sites on a simple cubic lattice. The interaction was limited to nearest neighbors and $S=1$. The exchange integral was a random variable characterized by a Gaussian distribution with zero mean and rms width equal to 1. The values for different bonds were uncorrelated.

In Figs. 1 and 2 we show the results for the average structure factor $S(\vec{q},E) = \frac{1}{3}\sum_{\alpha} S_{\alpha\alpha}(\vec{q},E)$, $\vec{q}$ along [100] and [111], for a $16\times16\times16$ lattice with periodic boundary conditions. The curves are normalized to unit area. The EC's were obtained by rotating the spins in the manner described in Refs. 1 and 2 and the integration was carried forward with the damping factor $\exp(-3t/T)$, with $T=40$.

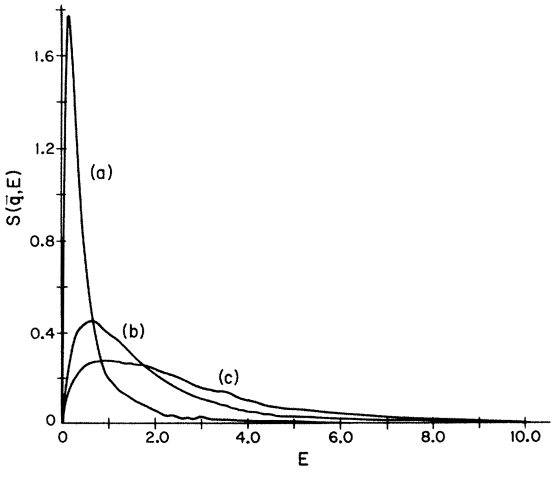

FIG. 1. $S(\vec{q},E)$ vs E. (a) $\vec{q}=(\pi/8)(1,0,0)$, (b) $\vec{q}=(\pi/2)(1,0,0)$, (c) $\vec{q}=\pi(1,0,0)$. $16\times16\times16$ simple cubic lattice with periodic boundary conditions. All curves normalized to unit area.

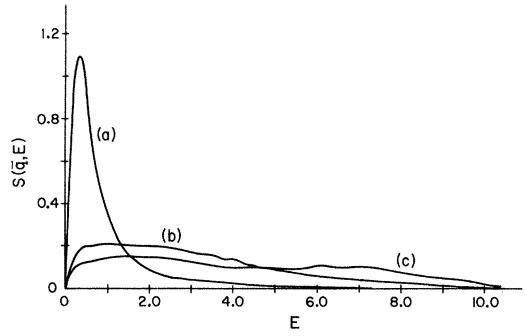

FIG. 2. $S(\vec{q},E)$ vs E. (a) $\vec{q}=(\pi/8)(1,1,1)$, (b) $\vec{q}=(\pi/2)(1,1,1)$, (c) $\vec{q}=\pi(1,1,1)$. $16\times16\times16$ simple cubic lattice with periodic boundary conditions. All curves normalized to unit area.

It is evident from the graphs that as $|\vec{q}| \rightarrow 0$ the spectral weight becomes increasingly concentrated near $E=0$. This is a consequence of the fact that

$$\vec{S}(\vec{q}=0) \cong (S/2)^{1/2} \sum_j (\vec{u}_j^{-} X_j + \vec{u}_j^{+} X_j^{\dagger})$$

is a constant of the motion (kinematic slowing down).[14] The interesting question is whether there is a well-defined peak in $S(\vec{q},E)$ at finite E which could be identified with a long-wavelength propagating mode.[7,8] Although such a peak is seen in the data at small q the figures are misleading. When the interval of integration in (2.23) is finite it is evident that $S(\vec{q},E)$ varies linearly with E for small E. As a consequence the sharp drop in $S(q,E)$ for $E \lesssim 0.05$ is an artifact of the numerical analysis. As evidence of this in Fig. 3 we show the behavior of

$$\frac{i}{\pi} \sum_{\alpha} \langle [S_{\alpha}(\vec{q},t), S_{\alpha}(-\vec{q},0)] \rangle \ ,$$

$\vec{q}=(\pi/8)\ (1,0,0)$, as a function of time [cf. Eq. (2.16)]. The function peaks at $t \simeq 5$ but shows no evidence of the oscillatory behavior characteristic of a weakly damped propagating mode.

It is perhaps worth noting that the curve in Fig. 3 can be fitted reasonably well by an approximation in which the sum over eigenstates in Eq. (2.16) is replaced by an integral over a Gaussian distribution, i.e.,

$$\sum_{\nu} |\langle 0|\, S_x(\vec{q},0)\,|\nu\rangle|^2 \sin(\omega_\nu t) \rightarrow \int_0^{\infty} \sin(\omega_\nu t)\, e^{-a_q \omega_\nu^2}\, d\omega_\nu \ . \tag{3.2}$$

The broken curve in Fig. 3 is calculated from the right-hand side of (3.2) with $a_q = 2.9$ and $A = 0.41$. Unfortunately the physical significance of this ap-

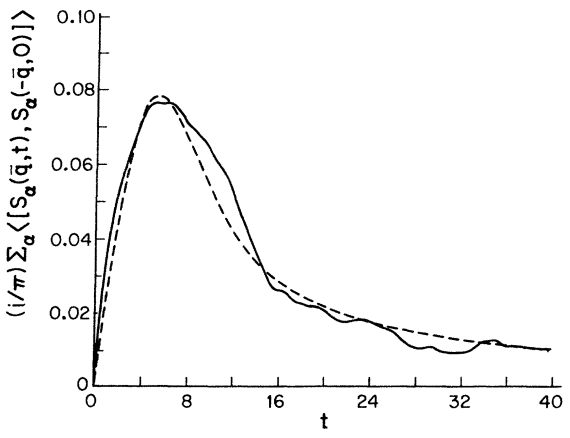

FIG. 3. $(i/\pi)\sum_\alpha\langle[S_\alpha(\vec{q},t),S_\alpha(-\vec{q},0)]\rangle$ vs t; $\vec{q}=(\pi/8)(1,0,0)$. $16\times16\times16$ simple cubic lattice with periodic boundary conditions. The broken line is an approximation displayed on the right-hand side of Eq. (3.2)

proximation is at present unclear. However taken at face value (3.2) would imply that

$$S(\vec{q},E)\propto e^{-a_q E^2}\quad (E>0)\ . \tag{3.3}$$

Since the intensity is peaked at $E=0$ Eq. (3.3) corresponds to a situation where the neutron scattering is quasielastic.

The left-hand side of (3.2) can also be written in the form

$$\int_0^\infty \rho(\omega_\nu)|\langle 0|S_x(\vec{q},0)|\nu\rangle|^2\sin(\omega_\nu t)\,d\omega_\nu\ , \tag{3.4}$$

where $\rho(\omega_\nu)$ is the density of states, which has been calculated numerically in Ref. 3. Since $\rho(E)$ has a peak at $E\approx2$ and approaches zero at low energies the apparent appropriateness of the Gaussian approximation would lead one to conclude that at long wavelengths $|\langle 0|S_\alpha(\vec{q},0)|\nu\rangle|^2$ peaks at (or near) $\omega_\nu=0$ and beyond that decreases rapidly with increasing mode energy.

It must be emphasized that the Gaussian form for $S(\vec{q},E)$ is a fairly crude approximation which is perhaps best viewed as a parametrization of the numerical data. Nevertheless it does indicate that a description in terms of weakly damped oscillatory modes is not appropriate for the wave vectors investigated.

IV. DISCUSSION

The results presented in the preceding section indicate the absence of propagating modes in $S(\vec{q},E)$ for $q\gtrsim\pi/8$. It is possible that such modes exist but are confined to energies and/or wave vectors very much smaller than can be probed by our numerical techniques which are limited to samples with fewer than 5×10^3 spins. Such a conclusion would be consistent with the findings of Reed[15] who reports a value for the spin-wave stiffness which is approximately 50% of the maximum value calculated below.

In order to obtain an estimate of the corresponding spin-wave velocity we note that the second moment of the normalized line-shape function $\chi''(\vec{q},E)/\pi E\chi(q)$, where $\chi(\vec{q},E)$ is the complex energy-dependent susceptibility, is given by[16]

$$\langle\omega_q^2\rangle=\frac{2}{3\chi(q)}\sum_{j,k}J_{jk}(1-\cos(\vec{q}\cdot\vec{r}_{jk}))\,\langle\vec{S}_j\cdot\vec{S}_k\rangle\ , \tag{4.1}$$

in which $\chi(q)$ is the wave-vector-dependent static susceptibility in units of $g^2\mu_B^2$, g being the electronic g factor. Passing to the small-q limit we find

$$\langle\omega_q^2\rangle=\left(\frac{1}{9\chi(0)}\sum_{j,k}J_{jk}r_{jk}^2\langle\vec{S}\cdot\vec{S}_k\rangle\right)q^2+O(q^4)\ . \tag{4.2}$$

Apart from the factor of $\chi(0)$ the coefficient of q^2 in (4.2) is the maximum spin-wave stiffness.[8,17] Values of the maximum stiffness and the uniform field susceptibility for the Edwards-Anderson model of Sec. III have been given in Ref. 7. Together they lead to the result

$$\langle\omega_q^2\rangle=(0.9\pm0.1)q^2+O(q^4)\ , \tag{4.3}$$

where length is measured in units of the lattice constant. The maximum spin-wave velocity is then given by

$$V_{\max}=(\lim_{q\to0}\langle\omega_q^2\rangle/q^2)^{1/2}\approx0.95\ . \tag{4.4}$$

Since the spin-wave velocity is equal to the square root of the ratio of the stiffness to the susceptibility, with a stiffness equal to one-half the maximum value we obtain

$$V=(0.5\lim_{q\to0}\langle\omega^2\rangle_q/q^2)^{1/2}\approx0.67\ . \tag{4.5}$$

Hence for $q=\pi/8$ the spin-wave peak is predicted to occur at $E\approx0.37$ which is somewhat greater than the position of the pseudopeak in Fig. 1. Thus had there been a peak in $S(\vec{q},E)$ at this energy and wave vector it would have been observed in our data.

Another possibility is that propagating modes are present but have negligible weight in the expansion of $S_\alpha(\vec{q})$ in terms of the eigenvectors of the dynamical matrix. In order to explore this possibility we have calculated the Green's function associated with the operator

$$X(\vec{q},t)=\sum_j\exp(-\vec{q}\cdot\vec{r}_j)X_j(t)\ . \tag{4.6}$$

Our results for the corresponding Green's function

$$(i/\pi)\langle[X(\vec{q},t),X^\dagger(\vec{q},0)]\rangle \tag{4.7}$$

are shown in Fig. 4 for $\vec{q}=(\pi/8)(1,0,0)$. In spite of

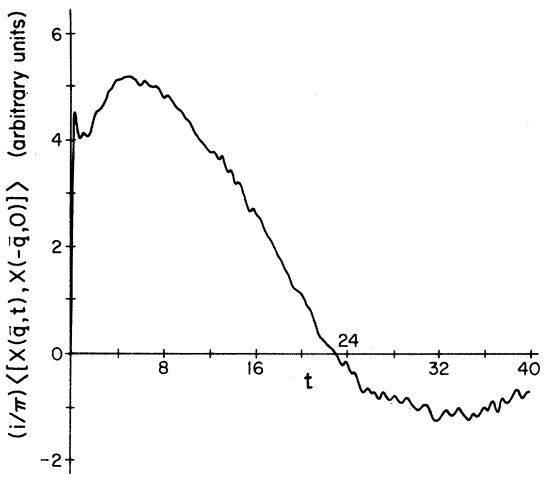

FIG. 4. $(i/\pi)\langle[X(\vec{q},t),X^{+}(\vec{q},0)]\rangle$ vs t; $\vec{q}=(\pi/8)(1,0,0)$. $16\times16\times16$ simple cubic lattice with periodic boundary conditions.

differing considerably from $(i/\pi)\langle[S_{\alpha}(\vec{q},t), S_{\alpha}(-\vec{q},0)]\rangle$, which is to be expected since $X(\vec{q}=0)$ is not a constant of the motion, $(i/\pi)\langle[X(\vec{q},t),X^{\dagger}(\vec{q},0)]\rangle$ also does not show the oscillations characteristic of weakly damped quasiharmonic behavior. Although this analysis does not rule out the existence of propagating modes which have negligible weight in the expansion of *both* $S_{\alpha}(\vec{q})$ and $X(\vec{q})$ the possibility of this occurring seems remote. Thus we conclude that there probably are no damped propagating spin-wave modes in the Edwards-Anderson model of a Heisenberg spin-glass which have wave vectors $q \gtrsim \pi/8$. Such modes, if they do exist, must have wave vectors $<< \pi/8$. The absence of propagating modes is also consistent with the behavior of the density of states at low energies which was displayed in Ref. 3. There it was found that the distribution of modes did not appear to have an E^2 dependence as would be the case if the low-frequency spectrum consisted entirely of propagating modes with a linear dispersion relation. However it should be emphasized that the absence of an E^2 dependence does not by itself rule out the existence of propagating modes since other types of low-energy excitations could also be present in large enough numbers to influence the distribution.

Our conclusions about the absence of weakly damped propagating modes with a linear dispersion relation are consistent with the findings of Krey who studied a $16\times16\times16$ model of $Eu_xSr_{1-x}S$.[11,12] For $x=0.4$, 0.5, and 0.6 (spin-glass phase) he found instead damped ferromagnetic spin waves in reasonable agreement with experiment.[18] Recently Fincher *et al.*[19] carried out inelastic neutron scattering studies on Fe_xCr_{1-x} ($x=0.34$ and 0.26) which revealed well-defined spin-wave modes in the ferromagnetic regime. The spin-wave stiffness decreased as the system was moved toward the spin-glass phase. In the spin-glass phase no well-defined excitations were seen. Instead an intense quasielastic peak analogous to what we obtained for the Edwards-Anderson model was observed.

The absence of propagating modes with wave vectors as small as $\pi/8$ in the Edwards-Anderson model is in distinct contrast to the behavior of the planar spin-glass[20,21] and the Heisenberg-Mattis model.[3,21–25] In both of these cases well-defined propagating modes with a linear dispersion relation were obtained in three dimensions for $q \lesssim \pi/4$. Although the two models differ radically in their equilibrium properties they have the common feature that the spin-wave dispersion relation at long wavelengths could be described in terms of a moderately renormalized virtual-crystal approximation (VCA).

In the VCA the dispersion relation is obtained by replacing the diagonal and off-diagonal elements of the dynamical matrix by the corresponding site-independent mean values. At long wavelengths the renormalized velocity is approximately $0.67\,V_{\rm VCA}$ for the planar model whereas in the case of the Heisenberg-Mattis model the value $0.81\,V_{\rm VCA}$ was obtained, $V_{\rm VCA}$ in both cases denoting the spin-wave velocity calculated in the VCA. It is perhaps worth noting that the model analyzed in Sec. III differs from the planar and Heisenberg-Mattis model in that the VCA applied to the dynamical matrix leads to a dispersion relation of the form

$$E(q)\approx[(3.7-0.7\gamma_q)^2-(0.7\gamma_q)^2]^{1/2}\ , \qquad (4.8)$$

with

$$\gamma_q=\tfrac{1}{3}(\cos q_x+\cos q_y+\cos q_z)\ , \qquad (4.9)$$

which does not vanish as $q\to0$. The term independent of γ_q in (3.8) is the mean value of the diagonal element of the matrix S_{jk} given by Eq. (2.5). It is identified as the precession frequency in the mean local field. Thus in the VCA the excitations are very nearly single spin modes. However the analysis of Ref. 3 indicates the modes are largely delocalized with a distribution which peaks at $E\approx2$.

In summary it can be said that the numerical techniques developed here and in Refs. 2 and 12 make it possible to obtain information about spin-wave dynamics in Heisenberg spin-glasses which is at least as detailed as that available experimentally. Unfortunately the theory of spin-wave dynamics has not kept pace with the numerical techniques. Unlike the case of the planar spin-glass[21] and the Heisenberg-Mattis model[22–24] there is as yet no satisfactory theory for the dynamic structure factor of a Heisenberg spin-glass.

ACKNOWLEDGMENTS

This research was supported by the NSF under Grant No. DMR-7904154. We would like to thank Dr. L. R. Walker and Dr. R. E. Walstedt for sending us reports of their unpublished work.

---

*Current address: Dept. of Phys., University of California-Santa Barbara, Santa Barbara, Calif. 93106.

[1]L. R. Walker and R. E. Walstedt, Phys. Rev. Lett. 38, 514 (1977).

[2]L. R. Walker and R. E. Walstedt, Phys. Rev. B 22, 3816 (1980).

[3]W. Y. Ching, K. M. Leung, and D. L. Huber, Phys. Rev. Lett. 39, 729 (1977).

[4]W. Y. Ching, D. L. Huber, and B. H. Verbeek, J. Appl. Phys. 50, 1715 (1979).

[5]W. Y. Ching, D. L. Huber, and K. M. Leung, Phys. Rev. B 21, 3708 (1980).

[6]W. Y. Ching and D. L. Huber (unpublished).

[7]D. L. Huber and W. Y. Ching, in *Amorphous Magnetism,* edited by R. A. Levy and R. Hasegawa (Plenum, New York, 1977), p. 39.

[8]B. I. Halperin and W. M. Saslow, Phys. Rev. B 16, 2154 (1977). See also K. H. Fischer, Z. Phys. B 39, 37 (1980), and references therein; W. M. Saslow, Phys. Rev. B 22, 1174 (1980); P. Rusek, Fiz. Tverd. Tela (Leningrad) 22, 1340 (1980) [Sov. Phys. Solid State 22, 783 (1980)].

[9]R. Alben and M. F. Thorpe, J. Phys. C 8, L275 (1975).

[10]M. F. Thorpe and R. Alben, J. Phys. C 9, 2555 (1976).

[11]U. Krey, J. Magn. Magn. Mater. 15–18, 123 (1980).

[12]U. Krey, Z. Phys. B 38, 243 (1980); and (unpublished).

[13]S. F. Edwards and P. W. Anderson, J. Phys. F 5, 965 (1975).

[14]Ref. 2, Appendix A.

[15]P. Reed, J. Phys. C 12, L475 (1979). Recently, R. E. Walstedt (private communication) has obtained a numerical estimate for the spin-wave stiffness in *Cu*Mn which is less than one-tenth of the "upper limit" estimated in Refs. 7 and 8.

[16]W. Marshall and R. D. Lowde, Rep. Prog. Phys. 31, 705 (1968).

[17]S. L. Ginsburg, Zh. Eksp. Teor. Phys. 75, 1497 (1978) [Sov. Phys. JETP 48, 756 (1978)].

[18]H. Maletta, W. Zinn, H. Schever, and S. M. Shapiro, in *26th Annual Conference on Magnetism and Magnetic Materials, Dallas, Texas, November 1980* [J. Appl. Phys. (in press)].

[19]C. R. Fincher, Jr., S. M. Shapiro, A. H. Palumbo, and R. D. Parks, Phys. Rev. Lett. 45, 474 (1980). Quasielastic scattering is also observed in the spin-glass phase of *Cu*Mn [H. Scheuer, J.-B. Suck, A. P. Murani, and M. Loewenhaupt, J. Magn. Magn. Mater. 14, 241 (1979); B. Dorner, A. P. Murani, and H. Scheuer, *ibid.* 14, 218 (1979)]. In making comparisons between experiment and harmonic spin-wave theory it is important to divide out the detailed balance factor, $(1-e^{-E/k_BT})^{-1}$, from the data so as to make direct contact with the zero-temperature dynamic structure factor [cf. Eq. (2.13)].

[20]D. L. Huber, W. Y. Ching, and M. Fibich, J. Phys. C 12, 3535 (1979).

[21]D. L. Huber and W. Y. Ching, J. Phys. C 13, 5579 (1980).

[22]D. Sherrington, J. Phys. C 10, L7 (1977).

[23]D. Sherrington, Phys. Rev. Lett. 41, 1321 (1978).

[24]D. Sherrington, J. Phys. C 12, 5171 (1979).

[25]W. Y. Ching and D. L. Huber, Phys. Rev. B 20, 4721 (1979).